CHEMISTRY OF MATERIALS
Article

Chem. Mater. **2011,** *23,* 823–831 823
DOI:10.1021/cm102128g

Oligothiophene Tetracyanobutadienes: Alternative Donor−Acceptor Architectures for Molecular and Polymeric Materials†

Ted M. Pappenfus,*,‡ Deborah K. Schneiderman,‡ Juan Casado,*,§ Juan T. López Navarrete,§ M. Carmen Ruiz Delgado,§ Gianni Zotti,⊥ Barbara Vercelli,⊥ Matthew D. Lovander,‡ Lindsay M. Hinkle,# Jon N. Bohnsack,# and Kent R. Mann#

‡*Division of Science and Mathematics, University of Minnesota, Morris, Minnesota 56267, United States,* §*Department of Physical Chemistry, University of Málaga, Campus de Teatinos s/n, Málaga 29071, Spain,* ⊥*Istituto CNR per l'Energetica e le Interfasi, c.o. Stati Uniti 4, 35127 Padova, Italy, and* #*Department of Chemistry, University of Minnesota, Minneapolis, Minnesota 55455, United States*

Received July 29, 2010. Revised Manuscript Received September 29, 2010

Oligothiophene-substituted 1,1,4,4-tetracyanobutadienes (TCBDs) have been synthesized by [2 + 2] cycloaddition reactions between tetracyanoethylene and oligothiophene alkynes. The TCBD moiety is compared to other electron acceptors attached to dibutylterthiophene including dicyanovinyl (DCV) and tricyanovinyl (TCV). These donor−acceptor molecules (**TCBD-3T**, **DCV-3T**, and **TCV-3T**) show red-shifted absorption spectra relative to the unsubstituted oligothiophene as a result of intramolecular charge-transfer (ICT). Monosubstituted terthiophenes bearing the electron acceptors show both oxidation and reduction processes as characterized by cyclic voltammetry. Density functional theory (DFT) calculations are used to explain the electronic and redox properties of the materials. Electrochemical oxidation of a bis(terthienyl)-substituted TCBD molecule (**3T-TCBD-3T**) yields a conducting polymer exhibiting balanced ambipolar redox conduction with similar values for the oxidized and reduced states of the polymer (1×10^{-3} S cm^{-1}). Raman spectra of the asymmetric donor−acceptor materials are characterized by two intense bands characteristic of the aromatic and quinoidal regions in the conjugated π-system of the oligothiophene.

Introduction

Donor−acceptor (D−A) organic molecules and polymers are one of the most important classes of conjugated materials for use in a number of technological applications.[1] Of particular interest are the use of these materials in organic photovoltaics.[2] In these materials, electron-donating and electron-accepting groups are connected through a variety of architectures. The exact nature of the acceptor and donor can be tuned precisely to create a variety of materials with unique physical and chemical properties. Among the donors available, functional thiophene-based materials have attracted considerable interest in this field.[3] Oligothiophenes have been functionalized with many electron-withdrawing groups such as carbonyl,[4] nitro,[5] and perfluoroalkyl.[6]

A particular class of electron acceptors that has received considerable attention are cyano-based electron acceptors.[7] For example, we and others[8] have used the tricyanovinyl moiety in oligothiophenes such as **TCV-3T** to create materials displaying nonlinear optical behavior[9]

† Accepted as part of the "Special Issue on π-Functional Materials".

*Corresponding authors. Email: pappe001@morris.umn.edu (FAX: 320-589-6371; Phone: 320-589-6340); casado@uma.es.

(1) For example, see the following and references therein: (a) Pron, A.; Gawrys, P.; Zagorska, M.; Djurado, D.; Demadrille, R. *Chem. Soc. Rev.* **2010**, *39*, 2577–2632. (b) Zhu, Y.; Kulkarni, A. P.; Wu, P.-T.; Jenekhe, S. A. *Chem. Mater.* **2008**, *20*, 4200–4211.

(2) (a) Fischer, M. K R.; Wenger, S.; Wang, M.; Mishra, A.; Zakeeruddin, S. M.; Gratzel, M.; Bauerle, P. *Chem. Mater.* **2010**, *22*, 1836–1845. (b) Bredas, J.-L.; Norton, J. E.; Cornil, J.; Coropceanu, V. *Acc. Chem. Res.* **2009**, *42*, 1691–1699. (c) Chen, J.; Cao, Y. *Acc. Chem. Res.* **2009**, *42*, 1709–1718. (d) Roncoli, J. *Acc. Chem. Res.* **2009**, *42*, 1719–1730. (e) Heremans, P.; Cheyns, D.; Rand, B. P. *Acc. Chem. Res.* **2009**, *42*, 1740–1747.

(3) Mishra, A.; Ma, C.-Q.; Bauerle, P. *Chem. Rev.* **2009**, *109*, 1141–1276.

(4) Yoon, M.-H.; Kim, C.; Facchetti, A.; Marks, T. J. *J. Am. Chem. Soc.* **2006**, *128*, 12851–12869.

(5) (a) Casado, J.; Pappenfus, T. M.; Miller, L. L.; Mann, K. R.; Orti, E.; Viruela, P. M.; Pou-Amerigo, R.; Hernandez, V.; Lopez Navarrete, J. T. *J. Am. Chem. Soc.* **2003**, *125*, 2524–2534. (b) Pappenfus, T. M.; Raff, J. D.; Hukkanen, E. J.; Burney, J. R.; Casado, J.; Drew, S. M.; Miller, L. L.; Mann, K. R. *J. Org. Chem.* **2002**, *67*, 6015–6024.

(6) (a) Facchetti, A.; Mushrush, M.; Yoon, M.-H.; Hutchinson, G. R.; Ratner, M. A.; Marks, T. J. *J. Am. Chem. Soc.* **2004**, *126*, 13859–13874. (b) Facchetti, A.; Yoon, M.-H.; Stern, C. L.; Hutchinson, G. R.; Ratner, M. A.; Marks, T. J. *J. Am. Chem. Soc.* **2004**, *126*, 13480–13501.

(7) (a) Barclay, T. M.; Cordes, A. W.; MacKinnon, C. D.; Oakley, R. T.; Reed, R. W. *Chem. Mater.* **1997**, *9*, 981–990. (b) Melucci, M.; Barbarella, G.; Zambianchi, M.; Di Pietro, P.; Bongini, A. *J. Org. Chem.* **2004**, *69*, 4821–4828. (c) Zotti, G.; Zecchin, S.; Vercelli, B.; Berlin, A.; Casado, J.; Hernandez, V.; Ortiz, R. P.; Lopez Navarrete, J. T.; Orti, E.; Viruela, P. M.; Milian, B. *Chem. Mater.* **2006**, *18*, 1539–1545.

(8) (a) Pappenfus, T. M.; Hermanson, B. J.; Helland, T. J.; Lee, G. G. W.; Drew, S. M.; Mann, K. R.; McGee, K. A.; Rasmussen, S. R. *Org. Lett.* **2008**, *10*, 1553–1556. (b) Pappenfus, T. M.; Burand, M. W.; Janzen, D. E.; Mann, K. R. *Org. Lett.* **2003**, *5*, 1535–1538. (c) Bader, M. M.; Custelcean, R.; Ward, M. D. *Chem. Mater.* **2003**, *15*, 616–618.

(9) Casado, J.; Ruiz Delgado, M. C.; Rey Merchan, M. C.; Hernandez, V.; Lopez Navarrete, J. T.; Pappenfus, T. M.; Williams, N.; Stegner, W. J.; Johnson, J. C.; Edlund, B. A.; Janzen, D. E.; Mann, K. R.; Orduna, J.; Villacampa, B. *Chem.—Eur. J.* **2006**, *12*, 5458.

Published on Web 10/22/2010

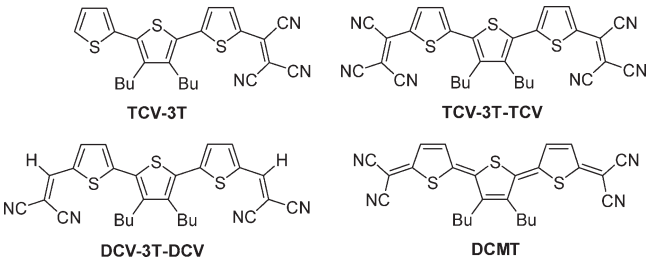

Figure 1. Representative cyano-based organic materials.

Scheme 1. Preparation of Donor-Substituted TCBDs

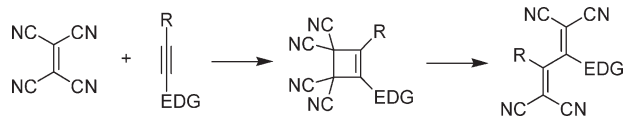

and **TCV-3T-TCV**, which exhibits n-type behavior in an organic thin-film transistor (Figure 1).[10] The first report of ambipolar transport in a thin-film transistor based on a single conjugated organic semiconductor was the dicyanomethylene material **DCMT**.[11] Additionally, Baeuerle and co-workers have utilized the dicyanovinyl moiety in materials such as **DCV-3T-DCV** for use in bulk heterojunction solar cells.[12] Given the promise of these and related materials, there is value in pursuing alternative cyano-based electron acceptors for use in π-conjugated materials.

Previously, Diederich and co-workers described that alkynes substituted with an electron-donating group (EDG) readily undergo a [2 + 2] cycloaddition with TCNE, followed by retro-electrocyclization to give charge transfer chromophores, donor-substituted 1,1,4,4-tetracyanobutadienes (TCBDs) as shown in Scheme 1.[13] This chemistry was later applied to a wide variety of electron-rich alkynes including bis-substituted alkynes.[14] These donor substituted TCBDs exhibit strong intramolecular charge transfer bands and strong electron accepting character as evidenced by electrochemical data. Although this rich chemistry has been applied to monomeric thiophenes, application to oligothiophenes has not yet been reported, to the best of our knowledge. Incorporating the strong TCBD acceptor with oligothiophenes is attractive because of the high ICT character of TCBD materials despite the nonplanarity of the group between the two dicyanovinyl planes. Additionally, unlike the previously reported cyano-based systems, TCBD materials have the ability to form bis-substituted molecules where R is also an electron donor such as an oligothiophene (Scheme 1). For example, when applied to a terthiophene, monomers of the type 3T-B-3T (where B is a linker) can be prepared and electropolymerized as some of us have previously investigated.[15] Utilization of TCBD as the linker is attractive as this introduces the possibility of both p- and n-doped polymers. This current research investigates the application of the TCBD electron-accepting group to both molecular and polymeric thiophene-based materials.

Experimental and Computational Details

General Considerations. Synthetic procedures were carried out under an inert atmosphere of nitrogen. Tetrahydrofuran and dichloromethane were distilled under a nitrogen atmosphere from Na/benzophenone and phosphorus pentoxide respectively. Acetonitrile was reagent grade (Uvasol, Merck) with a water content $< 0.01\%$. $Pd(PPh_3)_2Cl_2$ (Strem Chemicals Inc.) was purchased and used as received. The following were purchased from Aldrich and used as received: tetracyanoethylene, diisopropylamine, trimethylsilylacetylene, copper(I) iodide, 1,8-diazabicyclo[5.4.0]undec-7-ene (DBU), malononitrile, anhydrous benzene, and anhydrous *o*-xylene. Terthiophenes **1**[16] and **7**[17] were prepared as previously reported.

^{1}H NMR and ^{13}C NMR spectra were recorded on a JEOL Eclipse 300 MHz spectrometer. The chemical shifts are reported in ppm and referenced to the residual chloroform peak (7.26). Infrared spectra were recorded on a Bruker Tensor 27 FTIR spectrometer equipped with a Pike Technologies Miracle ATR accessory. Mass spectra were obtained on an in-house Agilent 5973 MSD mass spectrometer or on an Agilent ESI-MS at Scripps Center for Mass Spectrometry. Elemental analyses were performed by Atlantic Microlab, Inc., Norcross, GA.

Trimethyl(3′,4′-dibutyl-[2,2′:5′,2″-terthiophen]-5-ylethynyl)-silane (2). To a dry 100 mL Schlenk flask equipped with a magnetic stir bar was added **1** (0.750 g, 1.71 mmol), $Pd(PPh_3)_2Cl_2$ (0.0595 g, 0.0848 mmol), and copper(I) iodide (0.0170 g, 0.0893 mmol). The system was evacuated and backfilled with nitrogen three times. THF (10 mL) was added followed by the addition of diisopropylamine (0.76 mL, 5.4 mmol). To this solution was added trimethylsilylacetylene (0.41 mL, 2.9 mmol). The mixture was allowed to stir overnight at room temperature. The resulting suspension was filtered over diatoms and the solvent was removed via rotary evaporation. The resulting oil was purified by silica gel column chromatography (100% hexanes followed by 5% ethyl acetate in hexanes) to obtain 0.520 g (67%) of **2** as a citrine oil. ^{1}H NMR (300 MHz, $CDCl_3$): δ 7.32 (dd, 1H, J = 5.4, 1.2 Hz), 7.18 (d, 1H, J = 3.6 Hz), 7.14 (dd, 1H, J = 3.6, 1.2 Hz), 7.07 (dd, 1H, J = 5.1, 3.6 Hz), 6.98 (d, 1H, J = 3.9), 2.71 (m, 4H), 1.50 (m, 8H), 0.97 (m, 6H), 0.28 (s, 9H). ^{13}C NMR (75.6 MHz, $CDCl_3$): δ 140.73, 140.31, 138.05, 136.06, 133.20, 130.54, 129.35, 127.50, 126.13, 125.61, 125.38, 122.64, 100.07, 97.58, 33.00, 32.94, 28.04, 27.88, 23.10 (2C), 14.00, 13.96, 0.00 (3C). EI-MS m/z (relative intensity) 456 (100), 441 (4), 413 (12), 371 (12).

(10) Cai, X.; Burand, M. W.; Newman, C. R.; da Silva Filho, D. A.; Pappenfus, T. M.; Bader, M. M.; Bredas, J.-L.; Mann, K. R.; Frisbie, C. D. *J. Phys. Chem. B* **2006**, *110*, 14590.
(11) Chesterfield, R. J.; Newman, C. R.; Pappenfus, T. M.; Ewbank, P. C.; Haukaas, M. H.; Mann, K. R.; Miller, L. L.; Frisbie, C. D. *Adv. Mater.* **2003**, *15*, 1278–1282.
(12) Uhrich, C.; Schueppel, R.; Petrich, A.; Pfeiffer, M.; Leo, K.; Brier, E.; Kilickiran, P.; Baeuerle, P. *Adv. Funct. Mater.* **2007**, *17*, 2991–2999.
(13) Michinobu, T.; May, J. C.; Lim, J. H.; Boudon, C.; Gisselbrecht, J.-P.; Seiler, P.; Gross, M.; Biaggio, I.; Diederich, F. *Chem. Commun.* **2005**, 737–739.
(14) Michinobu, T.; Boudon, C.; Gisselbrecht, J.-P.; Seiler, P.; Frank, B.; Moonen, N. N. P.; Gross, M.; Diederich, F. *Chem.—Eur. J.* **2006**, *12*, 1889–1905.
(15) Zotti, G.; Vercelli, B.; Berlin, A.; Destri, S.; Pasini, M.; Hernandez, V.; Lopez Navarrete, J. T. *Chem. Mater.* **2008**, *20*, 6847–6856.
(16) (a) Araki, K.; Endo, H.; Masuda, G.; Ogawa, T. *Chem.—Eur. J.* **2004**, *10*, 3331–3340.(b) Pappenfus, T. M. Ph.D. Thesis, University of Minnesota, Minneapolis, MN, 2001.
(17) Pappenfus, T. M.; Melby, J. H.; Hansen, B. B.; Sumption, D. M.; Hubers, S. A.; Janzen, D. E.; Ewbank, P. C.; McGee, K. A.; Burand, M. W.; Mann, K. R. *Org. Lett.* **2007**, *9*, 3721–3724.

3′,4′-Dibutyl-5-ethynyl-2,2′:5′,2″-terthiophene (3). To a 2:1 dichloromethane:methanol solution (15 mL) of **2** (0.327 g, 0.716 mmol) was added K_2CO_3 (0.298 g, 2.16 mmol). This solution was stirred overnight before water (10 mL) was added. The aqueous layer was then extracted with dichloromethane (2 × 4 mL) and the organic layers combined. The organic layers were dried with $MgSO_4$, filtered and the solvent was removed by rotary evaporation to obtain 0.183 g (66.5%) of **3** as a viscous, dark-goldenrod colored oil. No further purification of this compound was performed. ^{1}H NMR (300 MHz, $CDCl_3$): δ 7.32 (dd, 1H, J = 5.1, 1.2 Hz), 7.23 (d, 1H, J = 3.9 Hz), 7.15 (dd,1H, J = 4.2, 1.2 Hz), 7.07 (dd, 1H, J = 5.4, 3.6 Hz), 7.00 (d, 1H, J = 3.9 Hz), 3.43 (s, 1H), 2.71 (m, 4H), 1.50 (m, 8H), 0.96 (m, 6H). ^{13}C NMR (75.6 MHz, $CDCl_3$): δ 140.88, 140.32, 138.38, 136.03, 133.55, 130.67, 129.14, 127.48, 126.18, 125.64, 125.35, 121.46, 82.34, 77.07, 33.00, 32.95, 28.05, 27.88, 23.11, 23.09, 13.96 (2C). EI-MS m/z (relative intensity) 384 (100), 341 (19), 299 (27).

TCBD-3T (4). A solution of TCNE (0.0527 g, 0.411 mmol) in benzene (7 mL) was added to **3** (0.144 g, 0.374 mmol) in benzene (4 mL) and stirred for 19 h at rt. The solvent was removed from the resulting deep violet solution via rotary evaporation. The resulting solid was dissolved in dichloromethane and purified by silica gel column chromatography (100% CH_2Cl_2) and washed with hexanes to obtain 0.113 g (58.9%) of **4** as a dark purple solid. ^{1}H NMR (300 MHz, $CDCl_3$): δ 7.96 (s, 1H), 7.69 (d, 1H, J = 4.2 Hz), 7.41 (dd, 1H, J = 5.0, 1.2 Hz), 7.35 (d, 1H, J = 4.5 Hz), 7.23 (dd, 1H, J = 3.6, 0.9 Hz), 7.11 (dd, 1H, J = 5.1, 3.6 Hz), 2.83 (t, 2H), 2.74 (t, 2H), 1.50 (m, 8H), 1.00 (t, 3H), 0.96 (t, 3H). IR (ATR) ν_{CN} (cm^{-1}): 2218. Anal. Calcd for $C_{28}H_{24}N_4S_3$: C, 65.59; H, 4.72; N, 10.93. Found: C, 65.66; H, 4.78; N, 10.78.

5,5‴-(1,2-Ethynediyl)bis-[3′,4′-dibutyl-2,2′:5′,2″-terthiophene] (5). To a dry 50 mL Schlenk flask equipped with a magnetic stir bar was added **1** (0.735 g, 1.67 mmol), $Pd(PPh_3)_2Cl_2$ (0.0704 g, 0.100 mmol), and copper(I) iodide (0.0319 g, 0.167 mmol). Anhydrous benzene (8.5 mL) was then added to the flask via syringe. Nitrogen-purged DBU (1.5 mL, 10.0 mmol) was added to the flask via syringe while the reaction flask was continued to purge with nitrogen. DI water was then added (12 μL, 0.67 mmol) to the flask via syringe and immediately ice-chilled trimethylsilylacetylene (118 μL, 0.835 mmol) was added by syringe. The nitrogen purge was removed from the reaction vessel and the Schlenk flask was sealed, placed in an oil bath at 80 °C, covered with foil to prevent exposure to light, and the mixture was stirred for 23 h. After cooling to room temperature, benzene (10 mL) and 3 M (aq) HCl (10 mL) were added to the flask with stirring. The layers were separated and the aqueous layer was extracted with benzene (2 × 6 mL). The organic fractions were combined, dried with $MgSO_4$, and filtered. The resulting crude material was adsorbed onto silica gel and purified using silica gel column chromatography (100% hexanes followed by 5% and 10% CH_2Cl_2 in hexanes) to provide 0.143 g (23.0%) of **5** as a bright yellow-orange solid. ^{1}H NMR (300 MHz, $CDCl_3$): δ 7.32 (dd, 2H, J = 5.0, 1.2 Hz), 7.23 (d, 2H, J = 3.9 Hz), 7.15 (dd, 2H, J = 3.5, 1.2 Hz), 7.07 (dd, 2H, J = 5.3, 3.6 Hz), 7.04 (d, 2H, J = 3.9 Hz), 2.72 (m, 8H), 1.49 (m, 16H), 0.96 (m, 12H). Anal. Calcd for $C_{42}H_{46}S_6$: C, 67.87; H, 6.24; S, 25.89. Found: C, 67.93; H, 6.20; S, 25.73.

3T-TCBD-3T (6). To a 50 mL two-necked round-bottom flask containing **5** (0.060 g, 0.081 mmol) and TCNE (0.0122 g, 0.0952 g) was added *o*-xylene (5 mL) via syringe. Heat was applied and the reaction was refluxed for 14 h with stirring under a nitrogen atmosphere. After cooling, the solvent was removed and the crude solid was purified by silica gel column chromatography (50:50 CH_2Cl_2:hexanes followed by 3:1 CH_2Cl_2:hexanes) to provide 0.049 g (70%) of **6** as a metallic green solid. ^{1}H NMR (300 MHz, $CDCl_3$): δ 7.77 (d, 2H, J = 4.7 Hz), 7.39 (dd, 2H, J = 5.4, 1.1 Hz), 7.30 (d, 2H, J = 4.4 Hz), 7.22 (dd, 2H, J = 3.9, 1.1 Hz), 7.10 (dd, 2H, J = 5.1, 3.9 Hz), 2.82 (t, 4H), 2.73 (t, 4H), 1.50 (m, 16H), 0.97 (m, 12H). IR (ATR) ν_{CN} (cm^{-1}): 2219. ESI-MS m/z: 871.2 $[M + H]^+$. Anal. Calcd for $C_{48}H_{46}N_4S_6$: C, 66.17; H, 5.32; N, 6.43. Found: C, 66.29; H, 5.34; N, 6.31.

DCV-3T (8). An ethanol solution (25 mL) containing **7** (0.233 g, 0.600 mmol), malononitrile (0.046 g, 0.70 mmol), and four drops of piperidine was refluxed for 18.5 h. The resulting solution was cooled and then 8 drops of concentrated hydrochloric acid were added. The solution was then returned to reflux for an additional 4.5 h. After cooling to room temperature the solution was concentrated via rotary evaporation. The crude material was purified by column chromatography (silica gel) using 1:1 CH_2Cl_2:hexanes. The pure fractions were combined and concentrated to provide 0.144 g (55.0%) of **8** as a red solid. ^{1}H NMR (300 MHz, $CDCl_3$): δ 7.76 (s, 1H), 7.68 (d, 1H, J = 3.9 Hz), 7.38 (dd, 1H, J = 5.1, 1.2 Hz), 7.27 (d, 1H, J = 4.5 Hz), 7.20 (dd,1H, J = 3.6, 1.2 Hz), 7.10 (dd, 1H, J = 5.1, 3.6 Hz), 2.79 (t, 2H), 2.72 (t, 2H), 1.50 (m, 8H), 0.99 (t, 3H), 0.96 (t, 3H). IR (ATR) ν_{CN} (cm^{-1}): 2221. EI-MS m/z (relative intensity) 436 (100), 351 (40). Anal. Calcd for $C_{24}H_{24}N_2S_3$: C, 66.01; H, 5.54; N, 6.42. Found: C, 66.19; H, 5.51; N, 6.21.

Spectroscopic Measurements of Oligomers. UV−vis spectra were recorded on an Ocean Optics USB HR4000 fiber optic spectrometer. Solution spectra were obtained in a 10 mm quartz cell. Thin film measurements were obtained by drop-casting onto glass or quartz from toluene or chloroform.

1064 nm FT−Raman spectra were measured using an FT−Raman accessory kit (FRA/106−S) of a Bruker Equinox 55 FT−IR interferometer. A continuous−wave Nd−YAG laser working at 1064 nm was used for excitation along with a germanium detector operating at liquid nitrogen temperature. Raman scattering radiation was collected in a back−scattering configuration with a standard spectral resolutions of 4 and 1 cm^{-1}. 1000−3000 scans were averaged for each spectrum.

Electrochemical Measurements. Room temperature electrochemical measurements were performed with a BAS 100B electrochemical analyzer and C3 cell stand in a three-electrode configuration with a glassy carbon working electrode (A = 0.07 cm^2), a platinum counter electrode, and a standard Ag|AgCl|KCl (1.0 M) reference electrode. A single compartment, low volume cell was used for all measurements. Tetrabutylammonium hexafluorophosphate electrolyte solution was added to the cell (5 mL, 0.1 M/CH_2Cl_2) and background cyclic voltammograms of the electrolyte solution were recorded prior to the addition of the sample. Suitable amounts of sample were added to create 0.5 mM solutions. The $E^{0\prime}$ values for the ferrocenium/ferrocene couple for concentrations similar to those used in this study were 0.43 V for dichloromethane solutions at a glassy carbon electrode. Anodic−cathodic peak separations were typically 80−90 mV for this redox couple.

The working electrode for the cyclic voltammetry of poly-(3T-TCBD-3T) films was a platinum (0.003 cm^2) minidisc electrode. For electronic spectroscopy of the polymer film, a 0.8 × 2.5 cm indium−tin-oxide (ITO) sheet (ca. 80% transmittance, ca. 20 ohm sq^{-1} resistance, from Kintec, Hong-Kong) was used. Electronic spectra were obtained with a Perkin-Elmer Lambda 5 spectrometer.

The apparatus and procedures used for the in situ conductivity experiments of the polymer were previously described in detail.[18,19] The electrode for conductivity measurements was a microband array platinum electrode (5 μm bandwidth, 100 nm thick) with interband spacing of 5 μm. The electrodeposited polymer was thick enough to cover the microband.

Single-Crystal X-ray Analysis of 5. A crystal (approximate dimensions $0.50 \times 0.28 \times 0.03$ mm^3) was placed onto the tip of a 0.1 mm diameter glass capillary and mounted on a Bruker SMART platform CCD diffractometer for a data collection at 173(2) K. The data collection was carried out using $Mo_{K\alpha}$ radiation (graphite monochromator) with a frame time of 45 s and a detector distance of 4.8 cm. The intensity data were corrected for absorption and decay.[20] Final cell constants were calculated from the xyz centroids of 4078 strong reflections from the actual data collection after integration.[21] The structure was solved and refined using SHELXL-97.[22] The terminal thiophene unit exhibits ring flip disorder and was modeled over two positions (relative occupancies of 92 and 8%). Each of the two thiophene disorder components are planar but twisted approximately 6.1° from one another. The disorder does not result in an increased number of interactions, nor does it direct the packing of the molecules within the crystal structure. Please refer to Table S1 in the Supporting Information for additional crystal and refinement information.

Computational Details. Density functional theory (DFT) calculations were performed with the Gaussian 03 program.[23] Geometries and orbital energies were calculated by means of the hybrid density functional B3LYP[24,25] with the basis set of 6-31G(d,p).[26−28] The input files were generated with GaussView. The ionization potentials (IPs) and electron affinities (EAs) were calculated directly from the relevant points on the potential energy surfaces using the standard procedure detailed in the literature.[29]

Scheme 2. Preparation of Mono-Terthienyl-Substituted Alkynes and TCBDs

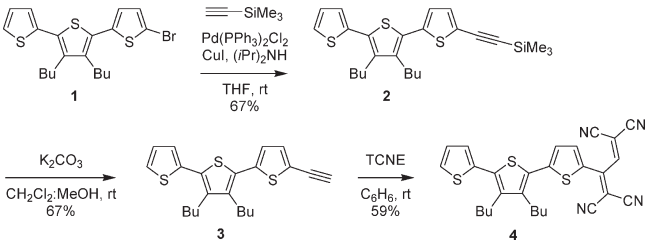

Scheme 3. Preparation of Bis-Terthienyl-Substituted Alkynes/TCBDs and Dicyanovinyl Oligomer

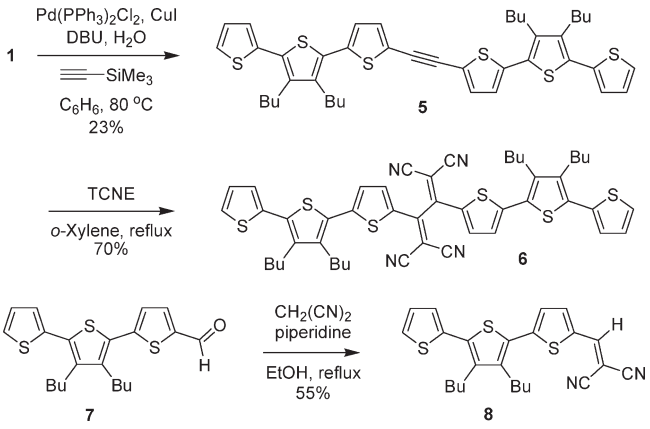

Results and Discussion

Synthesis. Schemes 2 and 3 illustrate the synthetic approaches to oligothiophene-TCBD materials and the related dicyanovinyl oligomer. The synthesis of the tricyanovinyl homologue **TCV-3T** has been reported previously.[9] The terminal alkyne **3** was prepared by methods previously described using Sonogashira coupling followed by protodesilylation with potassium carbonate (Scheme 2).[30] Addition of TCNE to **3** at room temperature afforded the mono-oligothiophene-substituted tetracyanobutadiene **TCBD-3T** (**4**) in 59% yield. This synthetic strategy was adapted from those previously reported for donor-substituted TCBDs.[14,31]

To prepare the bis-terthienyl-substituted TCBD, the symmetric bis-terthienyl-alkyne **5** was targeted. This oligomer was prepared in a one-pot synthesis using modified Sonogashira coupling reaction conditions that have been applied previously to a number of aromatic halides (Scheme 3).[32] Initial efforts to convert alkyne **5** to the TCBD oligomer in refluxing benzene afforded the desired product in low yield. Performing the reaction in *o*-xylene, however, significantly improved the reaction yield for the preparation of **3T-TCBD-3T** (**6**). Knoevenagel condensation was used to prepare **DCV-3T** (**8**) from **7**, utilizing a method previously reported for thiophene-DCV materials.[33]

(18) Aubert, P. H.; Groenendaal, L.; Louwet, F.; Lutsen, L.; Vanderzande, D.; Zotti, G. *Synth. Met.* **2002**, *126*, 193.
(19) Zotti, G.; Zecchin, S.; Vercelli, B.; Berlin, A.; Grimoldi, S.; Pasini, M. C.; Raposo, M. M. M. *Chem. Mater.* **2005**, *17*, 6492.
(20) Blessing, R. *Acta Crystallogr., Sect. A* **1995**, *51*, 33–38.
(21) *SAINT+ V6.45*; Bruker Analytical X-Ray Systems: Madison, WI, 2003.
(22) *SHELXTL V6.14*; Bruker Analytical X-Ray Systems:Madison, WI, 2000.
(23) Frisch, M. J.; Trucks, G. W.; Schlegel, H. B.; Scuseria, G. E.; Robb, M. A.; Cheeseman, J. R.; Montgomery, J. A., Jr.; Vreven, T.; Kudin, K. N.; Burant, J. C.; Millam, J. M.; Iyengar, S. S.; Tomasi, J.; Barone, V.; Mennucci, B.; Cossi, M.; Scalmani, G.; Rega, N.; Petersson, G. A.; Nakatsuji, H.; Hada, M.; Ehara, M.; Toyota, K.; Fukuda, R.; Hasegawa, J.; Ishida, M.; Nakajima, T.; Honda, Y.; Kitao, O.; Nakai, H.; Klene, M.; Li, X.; Knox, J. E.; Hratchian, H. P.; Cross, J. B.; Adamo, C.; Jaramillo, J.; Gomperts, R.; Stratmann, R. E.; Yazyev, O.; Austin, A. J.; Cammi, R.; Pomelli, C.; Ochterski, J. W.; Ayala, P. Y.; Morokuma, K.; Voth, G. A.; Salvador, P.; Dannenberg, J. J.; Zakrzewski, V. G.; Dapprich, S.; Daniels, A. D.; Strain, M. C.; Farkas, O.; Malick, D. K.; Rabuck, A. D.; Raghavachari, K.; Foresman, J. B.; Ortiz, J. V.; Cui, Q.; Baboul, A. G.; Clifford, S.; Cioslowski, J.; Stefanov, B. B.; Liu, G.; Liashenko, A.; Piskorz, P.; Komaromi, I.; Martin, R. L.; Fox, D. J.; Keith, T.; Al-Laham, M. A.; Peng, C. Y.; Nanayakkara, A.; Challacombe, M.; Gill, P. M. W.; Johnson, B.; Chen, W.; Wong, M. W.; Gonzalez, C.; Pople, J. A. *Gaussian 03*; revision C.02; Gaussian, Inc.: Wallingford, CT, 2004.
(24) Becke, A. D. *J. Chem. Phys.* **1993**, *98*, 5648.
(25) Lee, C. T.; Yang, W. T.; Parr, R. G. *Phys. Rev. B* **1988**, *37*, 785.
(26) Harihara, P. C.; Pople, J. A. *Theor. Chim. Acta* **1973**, *28*, 213.
(27) Hehre, W. J.; Ditchfield, R.; Pople, J. A. *J. Chem. Phys.* **1972**, *56*, 2257.
(28) Francl, M. M.; Pietro, W. J.; Hehre, W. J.; Binkley, J. S.; Gordon, M. S.; Defrees, D. J.; Pople, J. A. *J. Chem. Phys.* **1982**, *77*, 3654.
(29) Brédas, J. L.; Beljonne, D.; Coropceanu, V.; Cornil, J. *Chem. Rev.* **2004**, *104*, 4971.
(30) Pappenfus, T. M.; Mann, K. R. *Org. Lett.* **2002**, *4*, 3043–3046.
(31) Michinobu, T. *J. Am. Chem. Soc.* **2008**, *130*, 14074–14075.
(32) Mio, M. J.; Kopel, L. C.; Braun, J. B.; Gadzikwa, T. L.; Hull, K. L.; Brisbois, R. G.; Markworth, C. J.; Grieco, P. A. *Org. Lett.* **2002**, *4*, 3199–3202.
(33) Nesterov, E. E.; Skoch, J.; Hyman, B. T.; Klunk, W. E.; Bacskai, B. J.; Swager, T. M. *Angew. Chem., Int. Ed.* **2005**, *44*, 5452–5456.

Table 1. Spectroscopic and Electrochemical Data

molecule	λ_{max} (nm)[a]	λ_{max} (film) (nm)[b]	band gap (eV)[c]	E^{o}_{ox} (V)[d]	E^{o}_{red} (V)[d]
3T[e]	336	[f]	[f]	1.11[g]	[g]
TCV-3T	571	582	1.71	1.39[g]	−0.45, −1.13
TCBD-3T (4)	544	560	1.69	1.30[g]	−0.15, −0.78[h]
3T-TCBD-3T (6)	536	547	1.86	1.32[g]	−0.44, −0.63
DCV-3T (8)	474	502	2.12	1.28[g]	−1.06[h]

[a] Measured in dry CH_2Cl_2. [b] Sovent-cast film. [c] Optical. [d] Potentials vs Ag/AgCl in 0.1 M $TBAPF_6/CH_2Cl_2$ solution. [e] 3′,4′-Dibutyl-2,2′:5′,2″-terthiophene. [f] Compound is an oil. [g] Irreversible process; E_{pa} value provided. [h] Irreversible process; E_{pc} value provided.

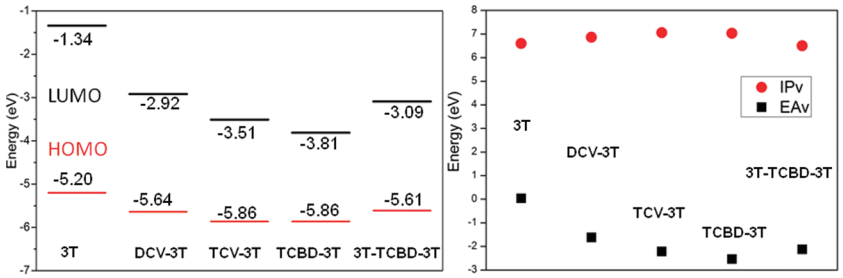

Figure 2. Left: Calculated HOMO and LUMO levels. Right: Vertical Ionization potentials (IPv) and electron affinities (EAv) for **3T** (3′,4′-dibutyl-2,2′:5′,2″-terthiophene) and related molecules.

The structure and purity of the TCBD and DCV materials were confirmed with NMR coupled with mass spectrometry and/or combustion analysis. Although we have been unsuccessful in obtaining suitable crystals of these materials for single-crystal X-ray analysis, we have been able to determine the X-ray structure of alkyne **5**. The ORTEP plot of **5** is shown in the Supporting Information (Figure S1). A crystallographic inversion center exists within the alkyne bridge of the molecule. Deviations from planarity exist within the molecule with the exception of the thiophene-ethyne-thiophene bridge which exhibits small deviations from planarity. Similar to the packing of the related tetrabutylsexithiophene[34] molecule, no π-stacking is present in **5** (packing views of the molecule are found in the Supporting Information).

UV−Vis Absorption and Electrochemical Properties. UV−vis absorption and cyclic voltammetry (CV) data of the various molecules are summarized in Table 1. Consistent with previous results of TCV-substituted oligothiophenes,[8,9] addition of electron-withdrawing DCV and TCBD groups result in dramatic red-shifts in the electronic spectra relative to the parent dibutylterthiophene (**3T**). For example, the lowest energy λ_{max} values increase across the **3T**/**DCV-3T**/**TCBD-3T**/**TCV-3T** series: 336 → 474 → 544 → 571 nm (see Figure S5 in the Supporting Information). Similar trends are seen in the thin film absorption data (Figure S6). This general trend has been previously attributed to the large stabilization of the LUMO by the electron withdrawing groups in oligothiophenes resulting in low energy intramolecular charge transfer electronic transitions.[5,9] Density functional theory (DFT) calculations at the B3LYP/6-31G-(d, p) level were performed for this series to illustrate this point (Figure 2). Although the HOMO levels are also stabilized in these molecules relative to **3T**, the magnitude of the LUMO stabilization is much greater resulting in a net reduction in HOMO−LUMO energy upon addition of the electron acceptor. The wave functions of the frontier molecular orbitals are depicted in Figure 3. As can be observed, the HOMO is delocalized along the whole π-conjugated backbone with the greatest contributions coming from the thiophene units while the LUMO is mostly concentrated on the cyano-based acceptor groups. These images provide further evidence of the ICT behavior of the materials (i.e., the HOMO → LUMO transition is a donor to acceptor intramolecular charge transfer).

Noteworthy is the comparison between the mono- and bis-substituted oligothiophene TCBDs. Addition of a second terthiophene to the TCBD moiety causes a blue-shift (**3T-TCBD-3T** λ_{max} = 536 nm) relative to **TCBD-3T** (λ_{max} = 544 nm). This feature has been rationalized by a substantial twist of the TCBD moiety upon the addition of a second group around the TCBD.[14] Geometry optimizations (see Figure S7 in the Supporting Information) confirm this feature where the torsion angle θ between the two dicyanovinyl planes is greater for the **3T-TCBD-3T** molecule. This molecular configuration causes a decrease in conjugation of the TCBD in **3T-TCBD-3T**, which elevates the LUMO level, thus creating a more energetic electronic transition.

The redox properties of this series of materials were investigated by CV (Table 1, Figure 4). The electrochemical data for **3T**[8b] and **TCV-3T**[9] were reported previously. Addition of one TCV group to the α-position of the **3T** chain results in the appearance of two reversible one-electron reductions for **TCV-3T**, and pushes the irreversible electrochemical oxidation of **3T** (1.11 V) to higher potential (1.39 V). Similar behavior is observed for the TCBD oligomers in this study and these data are consistent with those reported previously for donor-substituted TCBDs which also exhibit two one-electron reductions.[14]

(34) Liao, J. H.; Benz, M.; LeGoff, E.; Kanatzidis, M. G. *Adv. Mater.* **1994**, *6*, 135–138.

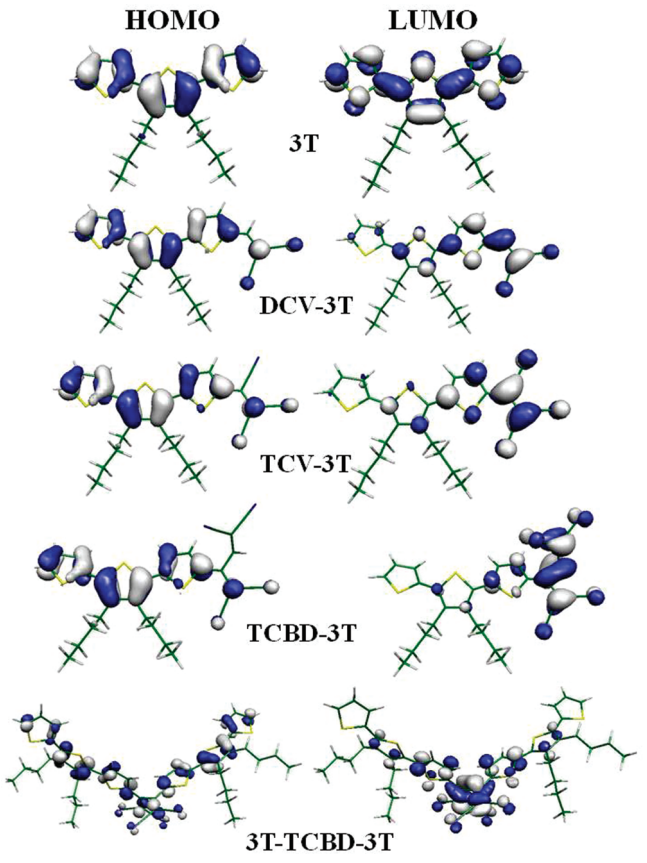

Figure 3. B3LYP/6-31G** wave functions of the frontier MOs in **3T** (3′,4′-dibutyl-2,2′:5′,2″-terthiophene) and related molecules.

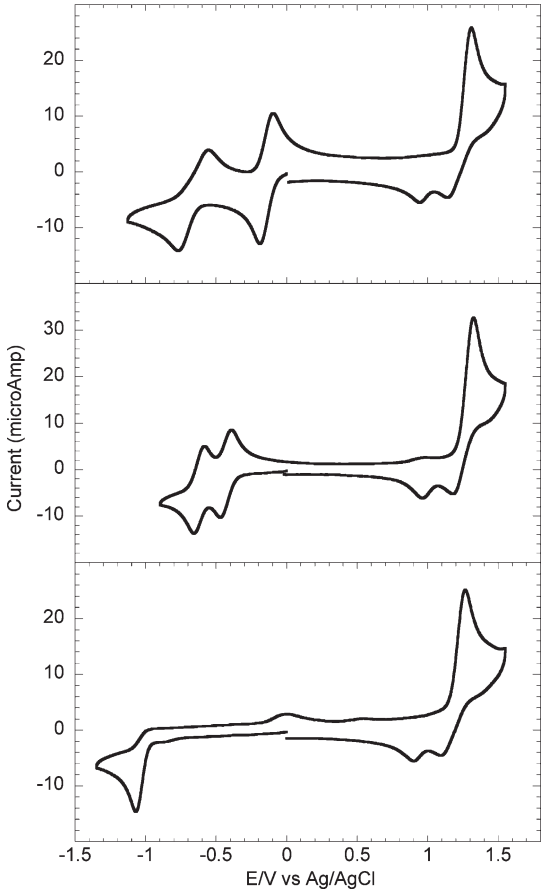

Figure 4. Cyclic voltammograms for **TCBD-3T** (top), **3T-TCBD-3T** (middle), and **DCV-3T** (bottom) in 0.1 M $TBAPF_6/CH_2Cl_2$ solutions at a carbon electrode, $\nu = 100$ mV/s.

These phenomena reflect the dual behavior of the TCV and TCBD groups regarding both the reduction (acting as an acceptor) and the oxidation (acting as an electron-withdrawing unit) processes when attached to terthiophene. Although **DCV-3T** also exhibits an irreversible oxidation at higher potentials relative to **3T**, addition of DCV to the terthiophene results in an irreversible reduction on the CV time scale. This behavior further supports utilizing DCV-oligothiophenes as electron donors rather than acceptors in device applications.[12]

Ionization potentials (IPs) and electron affinities (EAs) calculated at both Koopmans' theorem[35] (KT) and self-consistent-field (ΔSCF) levels are reported in Figure 2 and Table S2 in the Supporting Information. It is seen that the trends in the vertical ionization energies are well captured by the one-electron molecular orbital picture; that is, Koppmans' theorem applies well. When compared to unsubstituted terthiophene, the DFT-calculated vertical IPs increase upon acceptor substitution. On the other hand, the insertion of DCV, TCV, or TCBD groups to the terthiophene makes the EAs more exothermic, in the following order: **DCV-3T** (−1.62 eV) → **TCV-3T** (−2.21 eV) → **TCBD-3T** (−2.53 eV). This is in line with the overall stabilization of both the HOMO and the LUMO orbitals upon acceptor substitution (see Figure 2 for comparison purposes between the HOMO and LUMO energy levels and the EA/IP trends). These results are in very good agreement with the positive shift of the oxidation potential upon insertion of acceptor groups to the terthiophene (from 1.11 eV in **3T** to 1.28 eV in **DCV-3T**, 1.39 eV in **TCV-3T** and 1.30 eV in **TCBD-3T**) and with the first reduction potential evolution toward more positive values when the strength of the electron-withdrawing group increases (from −1.06 eV in **DCV-3T** to −0.45 eV in **TCV-3T** and −0.15 eV in **TCBD-3T**). It is interesting to note that insertion of an additional terthiophene unit in **3T-TCBD** causes a cathodic shift of the first reduction potential by 0.29 eV (−0.15 eV in **3T-TCBD** and −0.44 eV **3T-TCBD-3T**) which is in line with the less exothermic EA value calculated for **3T-TCBD-3T** (−2.12 eV) in comparison to **3T-TCBD** (−2.53 eV); this can be explained as a consequence of the greater twist between the two dicyanovinyl units of the TCBD group upon introduction of an additional terthiophene (vide supra).

Apart from the interesting optical and redox properties of the molecular materials, the architecture of the **3T-TCBD-3T** molecule and its potential to function as a monomer for polymeric materials prompted us to investigate its electrochemistry further. Repetitive scans in the CV experiment produced an increase in the current response (Figure 5) as an indication of polymer electrodeposition. According to the usual mechanism of coupling, the oxidation product is the α-coupled polymer, (**-6T-TCBD-**)$_n$ as illustrated in Scheme 4. The CV of

(35) Koopmans, T. *Physica* **1934**, *1*, 104–113.

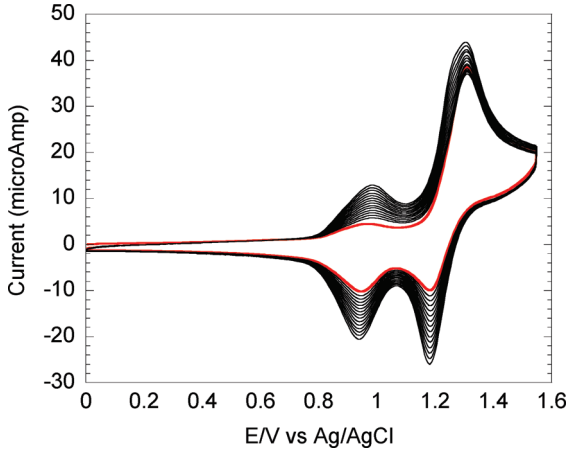

Figure 5. Repetitive CV scans (oxidative electropolymerization) of **3T-TCBD-3T** in 0.1 M $TBAPF_6/CH_2Cl_2$ at a carbon electrode, ν = 100 mV/s. First (red) through fifteenth scans shown.

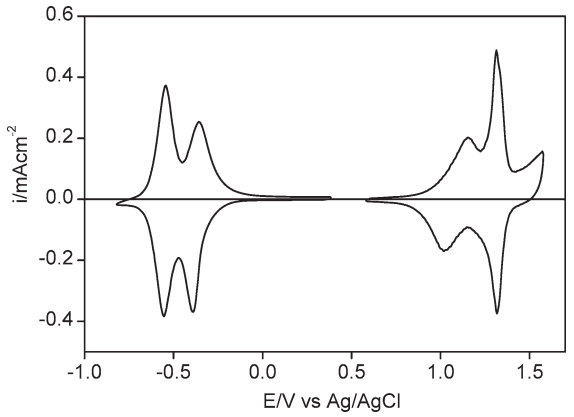

Figure 6. Cyclic voltammogram of **poly(3T-TCBD-3T)** film in 0.1 M $TBAPF_6/CH_3CN$ at a Pt electrode, ν = 100 mV/s.

Scheme 4. Anodic Coupling of 3T-TCBD-3T

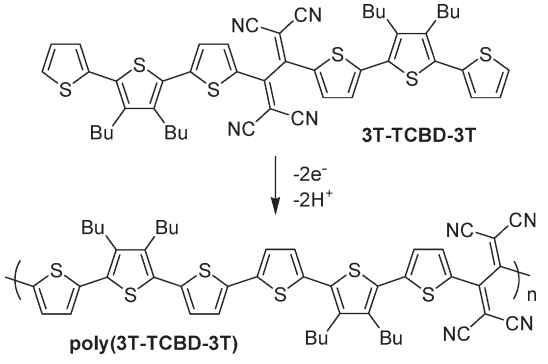

polymer deposits on a Pt electrode in acetonitrile shows two one-electron reduction waves at E^0 = −0.37 and −0.55 V, and oxidation waves at E^0 = 1.08 and 1.32 V (Figure 6). The spectrum of the polymer film on ITO (Figure 7) shows its maximum at 594 nm, red-shifted from that of the monomer in CH_2Cl_2 (536 nm). This indicates a more extended π-system is present in the polymer which results in a lower energy ICT.

The conductivity of **poly(3T-TCBD-3T)** as a function of the applied potential (Figure 8) displays peaks located

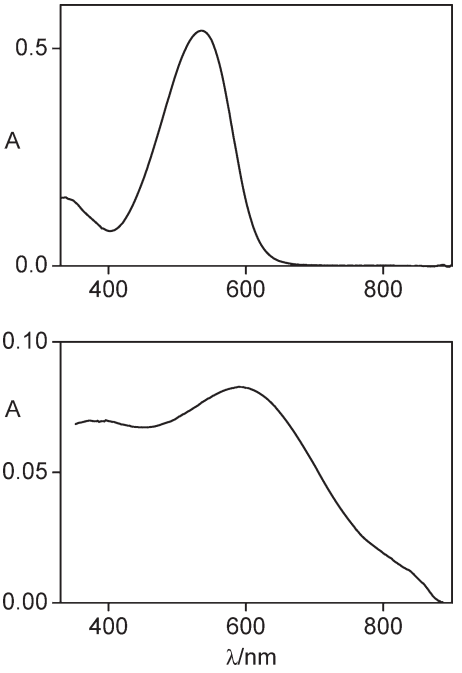

Figure 7. UV−vis spectra of **3T-TCBD-3T** in CH_2Cl_2 solution (top) and **poly(3T-TCBD-3T)** film on ITO (bottom).

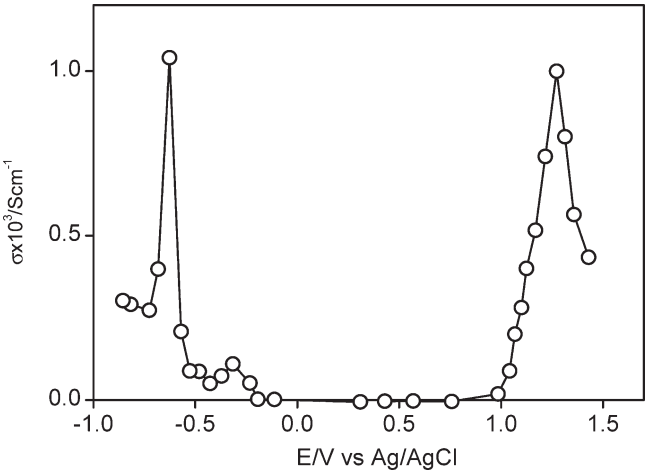

Figure 8. In situ conductivity of **poly(3T-TCBD-3T)** film in 0.1 M $TBAPF_6/CH_3CN$.

at 1.3 V for the oxidized form and at −0.6 V for the reduced form. This ambipolar conductivity is nearly identical for each process (ca. 1×10^{-3} S cm^{-1}) and is likely a simple redox conduction involving the anion-dianion and cation-dication couples. Although ambipolar transport has been previously reported in organic field-effect transistors for organic conjugated polymers,[36] examples of ambipolar redox conduction in electropolymerized films have not yet been reported to the best of our knowledge. Noteworthy, however, is the report by some of us on the molecular material **TCV-6T-TCV**, which exhibits both p- and n-channel transport in a thin film

(36) (a) Usta, H.; Risko, C.; Wang, Z.; Huang, H.; Deliomeroglu, J. K.; Zhukhovitskiy, A.; Facchetti, A.; Marks, T. J. *J. Am. Chem. Soc.* **2009**, *131*, 5586–5608. (b) Zaumseil, J.; Sirringhaus, H. *Chem. Rev.* **2007**, *107*, 1296–1323.

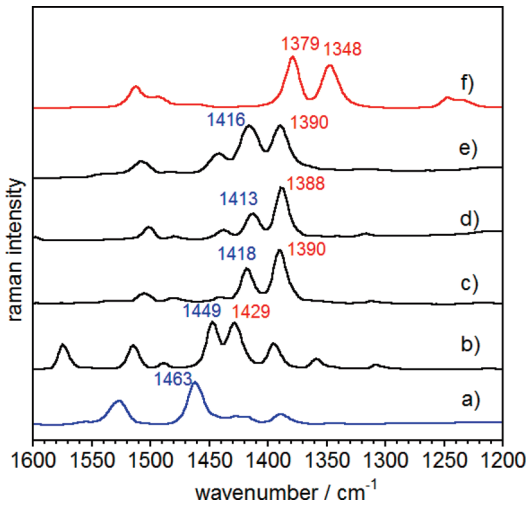

Figure 9. 1064 nm FT-Raman spectra of (a) **3T**, (b) **DCV-3T**, (c) **TCV-3T**, (d) **TCBD-3T**, (e) **3T-TCBD-3T**, and (f) **DCMT** in solid state.

transistor.[10] The structure of **TCV-6T-TCV** is similar to the backbone of **poly(3T-TCBD-3T)**, which may help explain conductive oxidized and reduced forms in both materials.

Vibrational Raman Spectra. The interpretation of vibrational Raman spectra of π−conjugated materials provides additional insight of donor−acceptor interactions in these materials. The 1064 nm FT-Raman spectra of the compounds are displayed in Figure 9. The most intense Raman band of **3T** appears at 1463 cm^{-1} and is due to a symmetric ν(C=C) mode spreading over the three rings (6 C=C and 5 C−C bonds). The rather similar π−conjugated structures of the three interacting thiophene rings in **3T** results in one unique Raman band which dominates the spectrum.[5a] The inclusion of the dicyanovinyl group in **DCV-3T** disrupts the symmetry and results in the appearance of two distinct and intense Raman bands both at lower frequencies (1449 and 1429 cm^{-1}) because of ν(C=C) modes located in substantially different ring moieties: one on the outermost (unsubstituted) thiophene ring corresponding to the vibration at 1449 cm^{-1} and one at the innermost (DCV-substituted) ring corresponding to the vibration at 1429 cm^{-1}. The rationale for this band splitting is the quinoidization caused by the electron-withdrawing character of the dicyanovinyl group. The ring directly connected to the DCV group adopts quinoidal character, whereas the outer thiophene maintains a predominantly aromatic structure.

The introduction of a third CN group in the case of **TCV-3T** produces a further frequency downshift of the intense band which is more pronounced for the substituted rings.[9] For example, for the **DCV-3T**→**TCV-3T** series, a 31 cm^{-1} shift (1449 → 1418) for the outer (unsubstituted rings) and a 39 cm^{-1} (1429 → 1390) shift for the substituted ring is observed. The attachment of a cross-conjugated tetracyanobutadiene pathway to the 3T moiety in the **TCBD-3T** molecule causes a slight frequency shift to lower values relative to **TCV-3T** in agreement with the overall greater electron-withdrawing property of the TCBD fragment.[13,14] Additionally, the occupation of the free position of **TCBD-3T** with an electron donor terthiophene produces **3T-TCBD-3T** and results in a frequency upshift in agreement with the reduced electron-acceptor character of the TCBD group when shared by two terthiophene groups. This effect simultaneously produces the π-electron decoupling of the two dicyanovinyl terthiophene moieties as discussed previously in the UV−vis section.

The structure−spectroscopy relationship indicates that depending on the proximity to the acceptor, the outermost thiophene rings display an aromatic-like structure, whereas the innermost ones display a quinoid-like structure.[37] This feature is demonstrated clearly by comparing the strong Raman band in the aromatic **3T** (1463 cm^{-1}) and in the completely quinoidal DCMT (1379 cm^{-1}) in Figure 9.[38] It is, however, important to differentiate between these two different situations. In the case of conventional aromatic oligothiophenes, a frequency downshift of the Raman band is observed with increasing π-conjugation. For example, in a complete series of thienyl aromatic compounds (i.e., with α,α′-dimethyl substitution) from bithiophene to sexithiophene, the intense Raman band changes from 1492 cm^{-1} in the former to 1477 cm^{-1} in the latter.[39] This downshift indicates a partial quinoidization of the molecular backbone together with an electron enrichment of the oligothiophene backbone, which is related to the decreasing first oxidation potential in this series of aromatic oligothiophenes. In the case of donor−acceptor oligothiophenes, the downshift in our cyano compounds (i.e., from 1449/1429 cm^{-1} in **DCV-3T** to 1413/1388 cm^{-1} in **TCBD-3T**) also means a progressive quinoidization of the π-conjugated structure occurs together with a decrease in the electron richness of the oligothiophene due to the electron-withdrawing effect of the cyano acceptor.

Conclusions

Addition of tetracyanoethylene to oligothiophene alkynes yields donor-substituted TCBD molecules in convenient one-step syntheses. Similar to oligothiophenes with dicyanovinyl and tricyanovinyl substitution, terthiophene tetracyanobutadienes exhibit strong intramolecular charge transfer bands in their absorption spectra. Unique features are also present in the Raman spectra of the donor−acceptor materials relative to unsubstituted oligomers. These TCBD oligothiophenes exhibit reversible reductions and irreversible oxidations on the CV time

(37) (a) Casado, J; Hernández, V.; Ruiz Delgado, M. C.; Ponce Ortiz, R.; López Navarrete, J. T.; Facchetti, A.; Marks, T. J. *J. Am. Chem. Soc.* **2005**, *127*, 13364–13372. (b) Casado, J.; Pappenfus, T. M.; Miller, L. L.; Mann, K. R.; Ortí, E.; Viruela, P. M.; Pou-AméRigo, R.; Hernández, V.; López Navarrete, J. T. *J. Am. Chem. Soc.* **2003**, *125*, 2524–2534.
(38) (a) Casado, J; Zgierski, M. Z.; Ewbank, P. C.; Burand, M. W.; Janzen, D. E.; Mann, K. R.; Pappenfus, T. M.; Berlin, A.; Perez-Inestrosa, E.; Ponce Ortiz, R.; López Navarrete, J. T. *J. Am. Chem. Soc.* **2006**, *128*, 10134–10144. (b) Casado, J.; Pappenfus, T. M.; Mann, K. R.; Orti, E.; Viruela, P. M.; Milián, B.; Hernandez, V.; Lopez Navarrete, J. T. *ChemPhysChem* **2004**, *5*, 529–539.
(39) Hernandez, V.; Casado, J.; Ramirez, F. J.; Zotti, G.; Hotta, S.; Lopez Navarrete, J. T. *J. Chem. Phys.* **1996**, *104*, 9271–9282.

scale. The irreversible processes allow for the formation of coupled products including the formation of the redox active conducting polymer, **poly(3T-TCBD-3T)**, which exhibits ambipolar redox conduction. The optoelectronic and redox properties of TCBD-oligothiophenes suggest they may be a readily accessible class of donor−acceptor materials for a number of electronic device applications.

Acknowledgment. T.M.P. acknowledges the following: (i) seed funding from the University of Minnesota Initiative for Renewable Energy and the Environment; (ii) University of Minnesota, Morris (UMM) Faculty Research Enhancement Funds supported by the University of Minnesota Office of the Vice President for Research and the UMM Division of Science and Mathematics for financial assistance; and (iii) Seth C. Rasmussen for his insight on electrochemical polymerizations and Paul C. Ewbank for the initial motivation to pursue this work. The authors also acknowledge the University of Minnesota X-ray Crystallographic Laboratory, Victor G. Young, Jr., P. Alex Rudd, and CHEM 5755. D.K.S. acknowledges the Morris Academic Partnership Program funded by the UMM Dean's Office. J.C. and J.T.L.N. are indebted to the Ministerio de Ciencia e Innovación through the project reference CTQ2009-10098 and to the Junta de Andalucia for the research project PO9-4708.

Supporting Information Available: Crystallographic information for molecule **5** (CIF); UV−vis absorption spectra and additional theoretical data (PDF). This material is available free of charge via the Internet at http://pubs.acs.org.